JOURNAL OF GUIDANCE, CONTROL, AND DYNAMICS
Vol. 32, No. 1, January–February 2009

Engineering Notes

ENGINEERING NOTES are short manuscripts describing new developments or important results of a preliminary nature. These Notes should not exceed 2500 words (where a figure or table counts as 200 words). Following informal review by the Editors, they may be published within a few months of the date of receipt. Style requirements are the same as for regular contributions (see inside back cover).

Experiments with Small Unmanned Helicopter Nose-Up Landings

S. Bayraktar*
Baykar Technologies, Istanbul, Turkey
and
E. Feron†
Georgia Institute of Technology, Atlanta, Georgia 30332-0150

DOI: 10.2514/1.36470

Nomenclature

g	=	gravitation constant
i_u, i_v	=	integral of horizontal velocity error
i_{v_z}	=	integral of vertical velocity error
k_{coll}	=	collective control proportionality constant
k_{du}, k_{dv}	=	helicopter horizontal aerodynamic drag coefficients
k_{i_u}, k_{i_v}	=	integral gains for horizontal velocity control loop
$k_{i_{v_z}}$	=	integral gain for vertical velocity control loop
$k_{\dot{z}}$	=	vertical drag coefficient
k_ϕ, k_θ, k_ψ	=	helicopter attitude control gains
m	=	helicopter mass
R	=	helicopter orientation (rotation matrix)
R_{cmd}	=	commanded orientation (rotation matrix)
R_{err}	=	orientation error (rotation matrix)
T_{coll}	=	helicopter rotor thrust
u, v	=	horizontal velocity in helicopter reference frame
u_{cmd}, v_{cmd}	=	commanded horizontal velocity in helicopter reference frame
V_{cmd}	=	commanded velocity amplitude
$V_{\max}$, $v_{z,\min}$, $v_{z,\max}$	=	velocity thresholds
v_x, v_y, v_z	=	helicopter speed in inertial reference frame
$v_{x,\text{cmd}}$, $v_{y,\text{cmd}}$, $v_{z,\text{cmd}}$	=	commanded velocity in inertial reference frame
$v_{x,\text{cmd},l}$, $v_{y,\text{cmd},l}$, $v_{z,\text{cmd},l}$	=	auxiliary commanded velocity in inertial reference frame
x, y, z	=	helicopter position in inertial reference frame
x_{cmd}, y_{cmd}, z_{cmd}	=	commanded position in inertial reference frame
x_{switch}	=	horizontal position threshold
δ_{roll}, δ_{pitch}	=	roll and pitch cyclic command inputs
δ_{rud}	=	rudder command input
ϵ_{err}	=	orientation error (rotation matrix logarithm)
λ_p, λ_z	=	proportional gains for position control loop
λ_u, λ_v	=	proportional gains for horizontal velocity control loop
λ_{v_z}	=	proportional gain for vertical velocity control loop
ϕ, θ, ψ	=	helicopter orientation (Euler angles)
ϕ_{cmd}, θ_{cmd}, ψ_{cmd}	=	commanded orientation (Euler angles)

I. Introduction

UNMANNED aerial vehicles have encountered growing popularity among civilian and military users alike, with hundreds of fixed-wing, unmanned aircraft operated every day throughout the world for surveillance and payload delivery missions [1]. With shrinking electronics size and increasing computer power, small airborne systems offer a wealth of new opportunities never imagined before the twenty-first century. The conjunction of growing interest for micro air vehicles with their easy operation in small, laboratory-sized environments has led academia and industry to launch many research efforts aimed at improving their agility and explore the boundaries of their flight envelope. It may rightfully be argued that high agility of small unmanned vehicles began with the era of missiles in the 1940s and 1950s. However, the novelty of the research opportunities offered by modern, small-sized machines is justified by the fact that many of them are expected to be recoverable and to be able to land and spend significant amounts of time within the theater of operations before taking off again, much like birds do in nature. As a result, there is a strong incentive to study the possibility for small machines not only to fly well and navigate properly during flight, but also to land in possibly constrained locations for the purpose of either replenishing their resources or performing a surveillance task. Words such as "perching" have become part of the popular jargon associated with such research activities, and much effort (discussed thereafter) has been devoted to performing landing maneuvers in constrained environments. Industry has leveraged the size of small fixed-wing unmanned vehicles to develop adapted recovery solutions such as Insitu's "skyhook" concept.‡ Similar developments are currently not available for small unmanned helicopters, despite their important operational relevance, and the need to expand the range of weather conditions for which landings are feasible, on a moving ship deck, for example.

Among noted and recent research contributions to the helicopter landing problem we find results from a control systems perspective [2–4] and from a vision-based sensing perspective [5,6]. Other teams have integrated control and vision together to demonstrate landings in various conditions [7–12], and there has also been significant

Received 4 January 2008; revision received 17 April 2008; accepted for publication 19 April 2008.

*Chief Scientist; selcuk.bayraktar@gmail.com.
†Professor, School of Aerospace Engineering; feron@gatech.edu. Associate Fellow AIAA.

‡Data available online at http://www.insitu.com/uas [retrieved 25 September 2008].

efforts aimed at understanding the landing strategies followed by bats and insects, in conjunction with their limited sensing capabilities [13–15]. However, the available experimental research literature focuses on autonomous helicopters landing on horizontal or quasi-horizontal surfaces: From a control systems perspective, the achieved vehicle performance does not differ much from technology available as far back as the 1950s.[§] On the side of theory, probably one of the most significant recent research concerns the control of tethered helicopters during landing [16], where the authors analyze the controlled dynamics of helicopters attached to a ship by means of a towing cable. On the side of operations, landing a helicopter on nonhorizontal terrain is considered to be a difficult task. According to experienced helicopter pilots, landing on sloped terrain requires slowly lowering the helicopter nacelle down to the ground, making sure that the rotor remains approximately horizontal as the nacelle slowly adjusts to local terrain orientation. This tends to produce significant structural stresses on the rotor of helicopters with semirigid or rigid hubs.

This Note focuses on the experimental demonstration of small helicopter landings at high nose-up attitudes (on surfaces inclined by as much as 60 deg) and the control methods used to achieve this result. Such a contribution is a useful intermediate step toward enabling all-attitude vehicle landing or alighting in geometrically constrained areas.

This Note is organized as follows. First, we describe the experimental setup used to perform the research, including the research vehicle, available instrumentation, and airspace layout. Then we briefly report human-in-the-loop experiments for helicopter landing on sloped platforms. The principles of automated vehicle landing are then presented, together with the control laws that were designed. Finally, experimental results are presented.

II. Experimental Setup

The experimental setup used for helicopter landing consists of 1) the flight test article, 2) the landing pad, and 3) the instrumentation system.

A. Flight Test Article

The flight test article chosen for the experiment is the Robbe Eolo Pro electric helicopter. This machine can be purchased for a relatively low price, making it a good candidate for experimentation. The technical specifications of the machine used for our experiments are given in Table 1. It can also be seen from the pictures that the rotor features Bell–Hiller stabilizer bars. In addition, the engine rpm is held constant using an on-board governor. For flight testing purposes, the helicopter has been modified as follows. First, the landing gear was modified to be compatible with the landing pad described thereafter. Second, the helicopter was painted with matte, gray paint to avoid unwanted reflections that would have interfered with the ground-based navigation system. Moreover, lightweight carbon rods were added to the landing gear. These rods support highly reflective beacons (see Fig. 1, right) used by the navigation system.

B. Instrumentation

A key element that enables aggressive maneuvers of small vehicles is the recent availability of reliable, ground-based navigation systems requiring only minimal on-board instrumentation. The VICON system[¶] provides such a turnkey navigation system. The system was originally designed to track human and animal motion. Its ground infrastructure consists of several cameras (typically six or more) which actively illuminate the tracked object via light-emitting diodes. With highly reflective coating over designated markers such as small-sized, styrofoam balls, the VICON system can track one or several rigid bodies in terms of position and orientation [17], provided the ambient light is low. For the purpose of avoiding any geometric ambiguity, it is important to place markers on the vehicle so as to break any symmetry (see Fig. 1). With such precautions taken and with an appropriate spatial distribution of the cameras, vehicle position and orientation can be obtained with position and attitude accuracy on the order of 1 cm and 1 deg, respectively, following a short calibration procedure. The sampling rate is 100 Hz and the latency is less than $1/25$ s.

Table 1 Helicopter characteristics

Main rotor diameter: 870 mm
Tail rotor diameter: 178 mm
All-up weight: 1300 g
Height: 256 mm
Length: 725 mm
Propulsion system: brushless electric motor
Medusa Research MR-028-056-2800

C. Landing Pad

The landing pad consists of a square 1.2×1.2 m^2 piece of plywood covered with Velcro. This piece of plywood can be easily tilted at various angles. Complementary Velcro material is mounted under the helicopter landing skids, so that upon contact the two elements (the landing pad and the helicopter landing gear) would effectively bond and notably eliminate the risk of helicopter overturn. Although it may be argued that such a solution creates artificially favorable conditions for successful landings, we consider that it constitutes a useful intermediate step toward performing landings in unequipped areas at nonhorizontal attitudes.

D. Experimental Layout

Flight tests were conducted in the courtyard of Georgia Institute of Technology's School of Aerospace. The VICON cameras were located in such a way that accurate position, velocity, attitude, and angular velocity information could be obtained for the helicopter in a corridor containing the helicopter initial position and the landing area. This corridor is 6 m deep, 1 m wide at maneuver inception, and greater than 3 m wide near the landing area. The available corridor height is about 3 m.

III. Experiments with Humans in the Loop

The first set of experiments involved an expert human pilot aiming at landing the helicopter on a moderately pitched target (25 deg). The human pilot was chosen for his ability to perform advanced aerobatic maneuvers (including inverted flight, loops, flips, rolls, etc.). The flight was performed at night as required by the VICON system. This challenged the pilot's ability to precisely locate the helicopter relative to the target. In particular, the strategy followed by the pilot to land the helicopter failed to exhibit many of the desired characteristics for landing at high pitch angles: The precise navigation requirements associated with helicopter landing forced the pilot to give up on adjusting the helicopter pitch angle so as to match that of the landing pad. Instead, the pilot chose to hover the helicopter horizontally above the landing pad and then dropped the helicopter on the pad by bringing the collective control down. This experiment showed that previously developed human-inspired strategies for aggressive flight control [18–21] could not be applied to the task described in this Note.

One of the benefits of the piloted experiments, however, was to demonstrate the validity of the "Velcro" landing pad concept, since the helicopter successfully and systematically bonded with the landing pad.

IV. Landing Maneuver Design

This section presents our landing maneuver design philosophy, followed by a detailed presentation of the control laws used to perform the maneuver.

[§]Data available online at http://www.gyrodynehelicopters.com/ or http://www.vtol.org/uavpaper/NavyUAV.htm [retrieved 25 September 2008].

[¶]Data available online at http://www.vicon.com [retrieved 25 September 2008].

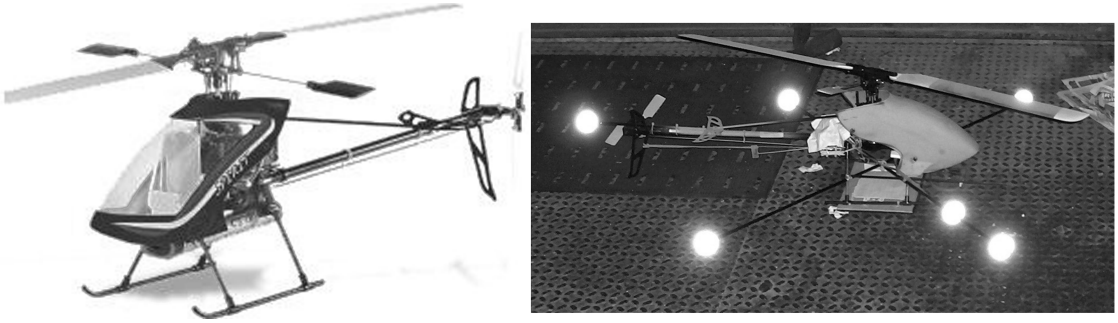

Fig. 1 Flight test article. Left: Commercial configuration. Right: Flight test configuration.

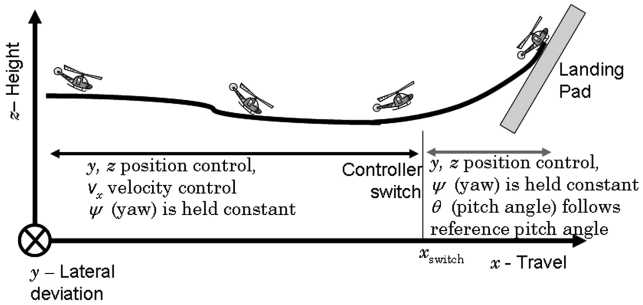

Fig. 2 Landing procedure.

A. Overall Philosophy

The landing maneuver was designed as a two-step process, illustrated by Fig. 2. What makes the landing maneuver challenging is the underactuated nature of the helicopter, where underactuated refers to the impossibility of controlling all degrees of freedom simultaneously. Indeed, assuming constant helicopter rotor speed, four actuation mechanisms are available (collective, pitch and roll, cyclic, and yaw). However, 6 degrees of freedom must be controlled (geometric position and attitude). Our landing maneuver is divided into two phases, as follows:

1) During approach, the lateral position y, altitude z, forward velocity $\dot{x}$, and yaw angle ψ of the helicopter are primarily controlled.

2) During flare and eventual landing, the pitch θ and yaw ψ angles of the helicopter are primarily controlled, together with the helicopter lateral position y and altitude z.

Thus, the vehicle undergoes a controller mode switch during the maneuver so as to enable the landing maneuver. This mode switch is reminiscent of strategies used in previous demonstrations of aerobatic flight by miniature helicopters [18,22]. The mode switch is triggered when the longitudinal vehicle position x crosses a specific threshold x_{switch}. During the experiments that led to this note, x_{switch} was determined empirically.

B. Recovery Procedure

The landing sequence was designed so that the vehicle could recover in case of a missed landing: Upon the crossing of a threshold distance $x_{\text{threshold}}$ or at the operator's discretion, the vehicle aborts its flight and is commanded to return to its starting point and hover there.

C. Control Architecture

The control architecture is given by the diagram in Fig. 3. Depending on the phase of the flight, only part or all of the controller architecture is used: For example, when hover control is desired, the entire control architecture is used. However, the vehicle forward velocity u may be commanded directly as well. Likewise, the helicopter pitch angle can be commanded directly. Three controllers are mounted in a series, corresponding to three successive loop closures. First, the *position controller* controls the forward and lateral motions of the helicopter, corresponding to the horizontal absolute coordinates x and y. The control laws (in terms of commanded speeds $v_{x,\text{cmd}}$, $v_{y,\text{cmd}}$, and $v_{z,\text{cmd}}$) are proportional laws subject to saturation. Define

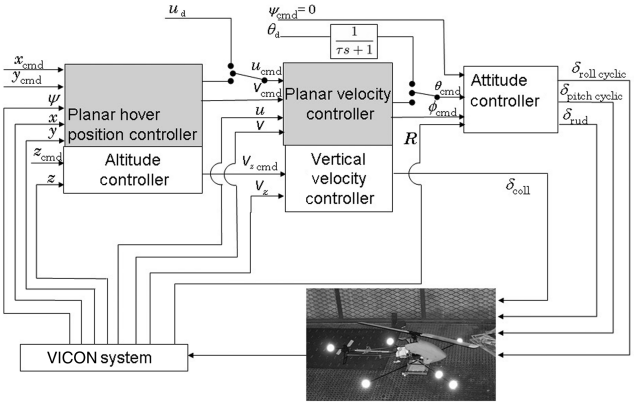

Fig. 3 Helicopter control architecture.

$$v_{x,\text{cmd},l} = -\lambda_p(x - x_{\text{cmd}}) \qquad v_{y,\text{cmd},l} = -\lambda_p(y - y_{\text{cmd}})$$
$$v_{z,\text{cmd},l} = -\lambda_z(z - z_{\text{cmd}}) \tag{1}$$

where x_{cmd}, y_{cmd}, and z_{cmd} are the commanded coordinates and x, y, and z are the measured coordinates of the helicopter in inertial coordinates. Defining

$$V_{\text{cmd}} = \sqrt{v_{x,\text{cmd},l}^2 + v_{y,\text{cmd},l}^2}$$

we then write

$$v_{x,\text{cmd}} = \frac{\text{SAT}(V_{\text{cmd}}/V_{\max})}{V_{\text{cmd}}/V_{\max}}\, v_{x,\text{cmd},l}$$
$$v_{y,\text{cmd}} = \frac{\text{SAT}(V_{\text{cmd}}/V_{\max})}{V_{\text{cmd}}/V_{\max}}\, v_{y,\text{cmd},l} \tag{2}$$
$$v_{z,\text{cmd}} = \min(\max(v_{z,\text{cmd},l}, v_{z,\min}), v_{z,\max})$$

The operator SAT is the usual saturation function. In practice, $V_{\max} = 1.5$ m/s, $v_{z,\min} = -1$ m/s, and $v_{z,\max} = 2$ m/s. The commanded velocities are then converted from an inertial frame of reference to the helicopter frame of reference:

$$\begin{bmatrix} u_{\text{cmd}} \\ v_{\text{cmd}} \end{bmatrix} = \begin{bmatrix} \cos\psi & \sin\psi \\ -\sin\psi & \cos\psi \end{bmatrix} \begin{bmatrix} v_{x,\text{cmd}} \\ v_{y,\text{cmd}} \end{bmatrix} \tag{3}$$

Alternatively, the forward velocity u_{cmd} may be controlled directly, as shown in Fig. 3. In these expressions, λ_p and λ_z are appropriately chosen positive constants.

The planar velocity command loop is computed as follows. A first-order velocity response is sought, such that

$$\frac{\text{d}}{\text{d}t}u = \lambda_u(u_{\text{cmd}} - u + i_u) \qquad \frac{\text{d}}{\text{d}t}v = \lambda_v(v_{\text{cmd}} - v + i_v)$$
$$\frac{\text{d}}{\text{d}t}i_u = k_{i_u}(u_{\text{cmd}} - u) \qquad \frac{\text{d}}{\text{d}t}i_v = k_{i_v}(v_{\text{cmd}} - v) \tag{4}$$

The presence of integrators (with states i_u and i_v) aims at guaranteeing zero tracking error. In these expressions, $\lambda_u, \lambda_v, k_{i_u}$, and

k_{i_v} are appropriately chosen positive constants. For control design purposes, we assume the simplified helicopter planar dynamics

$$\frac{\mathrm{d}}{\mathrm{d}t}u = \frac{1}{m}(-T_{\mathrm{coll}}\theta_{\mathrm{cmd}} + k_{\mathrm{du}}|u|u)$$
$$\frac{\mathrm{d}}{\mathrm{d}t}v = \frac{1}{m}(T_{\mathrm{coll}}\phi_{\mathrm{cmd}} + k_{\mathrm{dv}}|v|v) \tag{5}$$

where T_{coll} is the helicopter rotor thrust setting (collective), m is the mass of the helicopter, and the aerodynamic drag coefficients k_{du} and k_{dv} are computed by assuming the helicopter to be an ellipsoid [23,24]. This model is a considerable simplification of the more complex models found in the literature [25], but it is satisfactory for controller design purposes. Inverting the helicopter dynamics [26] leads to expressions for θ_{cmd} and ϕ_{cmd}

$$\theta_{\mathrm{cmd}} = -\frac{1}{T_{\mathrm{coll}}}(\lambda_u m(i_u + u_{\mathrm{cmd}} - u) - k_{\mathrm{du}}u|u|)$$
$$\phi_{\mathrm{cmd}} = \frac{1}{T_{\mathrm{coll}}}(\lambda_v m(i_v + v_{\mathrm{cmd}} - v) - k_{\mathrm{dv}}v|v|) \tag{6}$$

by combining Eqs. (4) and (5) together. Alternatively, the pitch angle θ may be directly commanded via the input θ_d. To avoid exciting the helicopter's high-frequency pitch dynamics, θ_d is subject to low-pass (first-order) filtering. Together with the desired heading ψ_{cmd}, the Euler angles θ_{cmd} and ϕ_{cmd} allow us to form the desired attitude, expressed by the rotation matrix R_{cmd} [27]. Computing the rotation error matrix $R_{\mathrm{err}} = R_{\mathrm{cmd}}^{-1}R = R_{\mathrm{cmd}}^{T}R$, where R is the measured orientation of the helicopter (obtained from the measured Euler angles ϕ, θ, and ψ), and computing $\epsilon_{\mathrm{err}} = \log R_{\mathrm{err}}$ [28], we obtain

$$\epsilon_{\mathrm{err}} = \begin{bmatrix} 0 & -\epsilon_z & \epsilon_y \\ \epsilon_z & 0 & -\epsilon_x \\ -\epsilon_y & \epsilon_x & 0 \end{bmatrix} \tag{7}$$

Standard results about rotations indicate that the orientation error R_{err} is a rotation whose axis is $[\epsilon_x \quad \epsilon_y \quad \epsilon_z]^T$ and whose angular amplitude is $\sqrt{\epsilon_x^2 + \epsilon_y^2 + \epsilon_z^2}$. The proportional control law

$$\delta_{\mathrm{roll}} = k_\phi \epsilon_x \qquad \delta_{\mathrm{pitch}} = k_\theta \epsilon_y \qquad \delta_{\mathrm{rud}} = k_\psi \epsilon_z \tag{8}$$

was chosen for its simplicity and ability to steer the helicopter attitude R toward R_{cmd}. Damping is provided by the helicopter dynamics, including the stabilizer bars and the built-in gyroscopic yaw damper.

The velocity controller about the z inertial axis was computed using the desired behavior

$$\frac{\mathrm{d}}{\mathrm{d}t}v_z = \lambda_{v_z}(v_{z,\mathrm{cmd}} - v_z + i_{v_z}) \qquad \frac{\mathrm{d}}{\mathrm{d}t}i_{v_z} = k_{i_{v_z}}(v_{z,\mathrm{cmd}} - v_z) \tag{9}$$

Using the simplified vertical dynamics

$$\dot{v}_z = \frac{1}{m}(T_{\mathrm{coll}}\cos\theta\cos\phi - mg - k_{\dot{z}}v_z) \tag{10}$$

and

$$T_{\mathrm{coll}} = k_{\mathrm{coll}}\delta_{\mathrm{coll}} \tag{11}$$

where $k_{\dot{z}}$ and k_{coll} are computed separately as functions of the rotor characteristics assuming the helicopter is near hover, yields the desired control law

$$\delta_{\mathrm{coll}} = \frac{mg + m\lambda_{v_z}(v_{z,\mathrm{cmd}} + i_{v_z} - v_z) + k_{\dot{z}}v_z}{k_{\mathrm{coll}}\cos\theta\cos\phi} \tag{12}$$

Such a control architecture enables a high-level, discrete control of the helicopter. The landing sequence may be seen as a discrete sequence of step inputs to the control architecture as shown in Fig. 4.

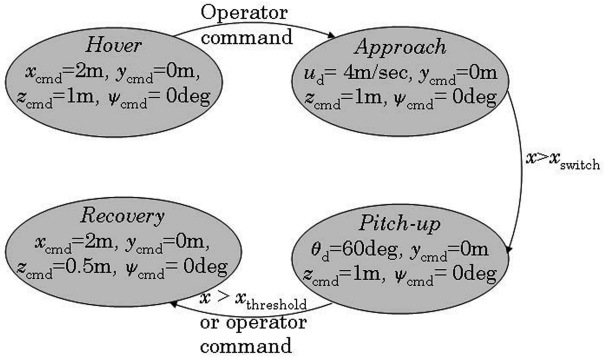

Fig. 4 Landing maneuver sequence.

V. Experimental Results

The controlled helicopter was able to perform several landings, eventually reaching a 60-deg pitch angle at landing. Initial landings were performed at much smaller pitch angles (e.g., 10 deg) for the purpose of calibrating the landing procedure and the abort process, should it be needed. The pitch angle of the landing pad was then progressively increased so as to eventually reach 60 deg. Figure 5 shows the trajectory followed by the helicopter during a successful landing.

The corresponding time histories for attitude/attitude rates and position/speeds are given in Figs. 6 and 7. It must be noted that the landing maneuver is, so far, performed "open loop," that is, the exact location of the landing pad relative to the helicopter was not measured in real time, leading to several aborted maneuvers. In addition, the orientation of the landing pad was not measured online. The operator measured the landing pad pitch angle before the flight, and entered it manually as θ_d in the flight control computer. During these experiments, the thresholds were set to be $x_{\mathrm{switch}} = 5.7$ m and $x_{\mathrm{abort}} = 7.85$ m. The actual landing took place at $x = 7.73$ m.

VI. Further Research

This Note shows that the concept of landing a small, unmanned hover-capable vehicle on a near-vertical surface is feasible. From there, several avenues of research are possible. First, it is necessary to improve the reliability and repeatability of the landing maneuvers, by improving the control laws used, and by sensing the proximity of the vehicle to the landing surface. Recently developed control strategies for helicopterlike vehicles might prove useful [29]. Second, the range of helicopter attitudes at landing should ideally be extended to incorporate all possible attitudes. Third, effective and reversible bonding mechanisms should be designed to replace the Velcro-based system used so far.

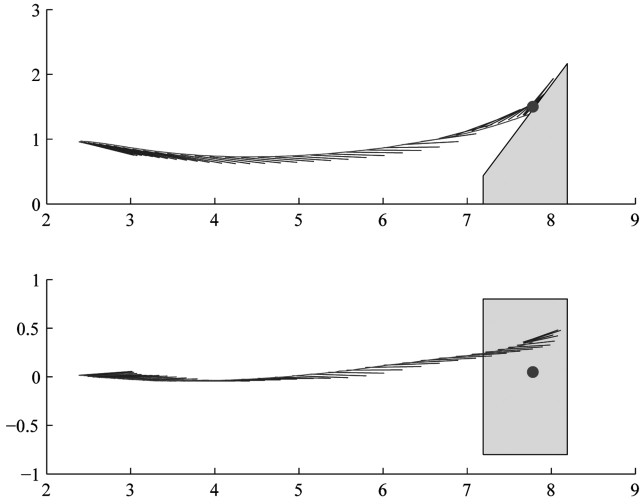

Fig. 5 Successful landing: Top: Side view. Bottom: Top view. Helicopter attitude is represented by successive segments. Consecutive segments are separated by 0.06 s. All units are in meters.

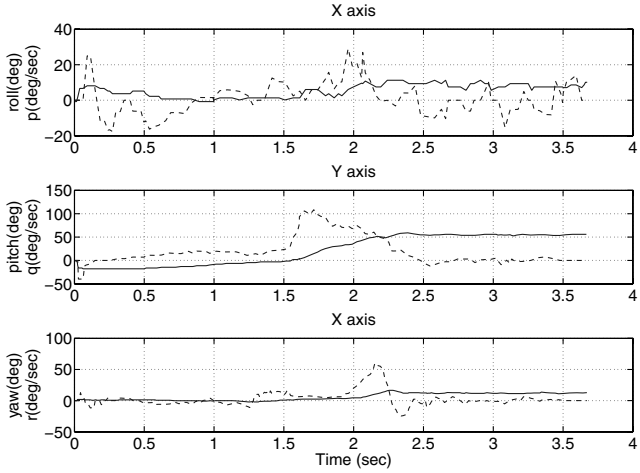

Fig. 6 Successful landing: Helicopter attitude/attitude rates. Angles are continuous lines; angular rates are dashed lines.

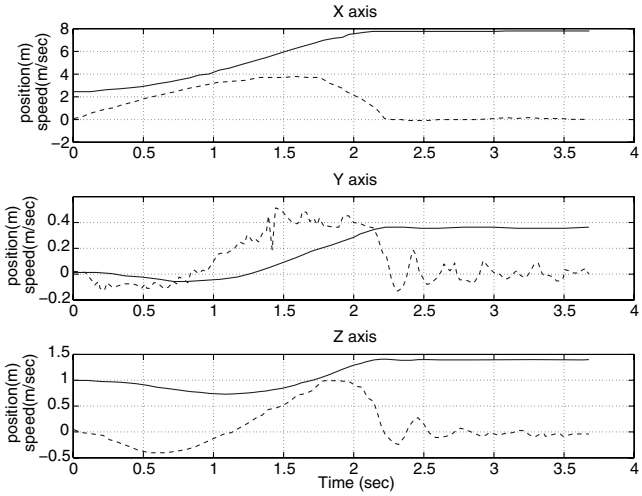

Fig. 7 Successful landing: Helicopter position/velocity. Top: Along track position/velocity; Middle: Cross-track position/velocity. Bottom: Altitude/vertical speed. Positions are continuous lines; velocities are dashed lines.

VII. Conclusions

This Note presented the first published landing of a small helicopter at high pitch angle, with landings on platforms with up to 60 deg pitch. Such maneuvers contribute to forming the core knowledge that is necessary to enable birdlike behaviors for small unmanned air vehicles, including the ability for these vehicles to alight at nonhorizontal attitudes. This interim result shows that these high-agility behaviors are now within reach of small unmanned air vehicles and navigation systems.

Acknowledgments

This research was supported by the Office of Naval Research under Grant N00014-06-1-1158. The authors would like to thank H. DeBlauwe, R. Cash, M. Gariel, T. Hunter, F. Lokumcu, M. Pakhmer, V. Stojanovska, R. Valenzuela, and the safety pilot J. Fine for their support during this effort.

References

[1] Wilson, J., "UAV Worldwide Roundup 2007," *Aerospace America*, No. 5, May 2007, pp. 30–37.

[2] Koo, T., and Sastry, S., "Output Tracking Control Design of a Helicopter Model Based on Approximate Linearization," *Proceedings of the IEEE Conference on Decision and Control*, Vol. 4, IEEE, Piscataway, NJ, Dec. 1998, pp. 3635–3640.

[3] Shim, H., Koo, T., Hoffmann, F., and Sastry, S., "A Comprehensive Study of Control Design for an Autonomous Vehicle," *Proceedings of the 37th IEEE Conference on Decision and Control*, Vol. 4, IEEE, Piscataway, NJ, Dec. 1998, pp. 3653–3658.

[4] Isidori, A., Marconi, L., and Serrani, A., "Robust Nonlinear Motion Control of a Helicopter," *IEEE Transactions on Automatic Control*, Vol. 48, No. 3, 2003, pp. 413–426. doi:10.1109/TAC.2003.809147

[5] Sharp, C., Shakernia, A., and Sastry, S., "A Vision System for Landing an Unmnanned Aerial Vehicle," *Proceedings of the IEEE International Conference on Robotics and Automation*, Vol. 2, IEEE, Piscataway, NJ, May 2001, pp. 1720–1727.

[6] Shakernia, O., Vidal, R., Sharp, C., Ma, Y., and Sastry, S., "Multiple View Motion Estimation and Control for Landing an Unmanned Aerial Vehicle," *Proceedings of the IEEE International Conference on Robotics and Automation*, Vol. 3, IEEE, Piscataway, NJ, May 2002, pp. 2793–2798.

[7] Saripalli, S., and Sukhatme, G., "Landing on a Moving Target Using an Autonomous Helicopter," *International Conference on Field and Service Robotics*, Vol. 24, Springer Tracts in Advanced Robotics, Springer, Berlin/Heidelberg, July 2006, pp. 277–286.

[8] Saripalli, S., Sukhatme, G., and Montgomery, J., "An Experimental Study of the Autonomous Helicopter Landing Problem," *Experimental Robotics VIII*, Vol. 5, Springer Tracts in Advanced Robotics, Springer, Berlin/Heidelberg, 2003, pp. 466–475.

[9] Garcia-Pardo, P., Sukhatme, G., and Montgomery, J. F., "Towards Vision-Based Safe Landing for an Autonomous Helicopter," *Robotics and Autonomous Systems*, Vol. 38, No. 1, 2002, pp. 19–29. doi:10.1016/S0921-8890(01)00166-X

[10] Corke, P., "An Inertial and Visual Sensing System for a Small Autonomous Helicopter," *Journal of Robotic Systems*, Vol. 21, No. 2, Feb. 2004, pp. 43–51. doi:10.1002/rob.10127

[11] Theodore, C., Sheldon, S., Rowley, D., McLain, T., Dai, W., and Takahashi, M., "Full Mission Simulation of a Rotorcraft Unmanned Aerial Vehicle for Landing in a Non-Cooperative Environment," *61st Annual Forum of the American Helicopter Society*, AHS International, Alexandria VA, June 2005.

[12] Tournier, G., Valenti, M., How, J., and Feron, E., "Estimation and Control of a Quadrotor Vehicle Using Monocular Vision and Moiré Patterns," AIAA Paper 2006-6711, Aug. 2006.

[13] Chahl, J., Srinivasan, M., and Zhang, S. W., "Landing Strategies in Honeybees and Applications to Uninhabited Airborne Vehicles," *International Journal of Robotics Research*, Vol. 23, No. 2, Feb. 2004, pp. 101–110. doi:10.1177/0278364904041320

[14] Tian, B., and Schnitzler, H.-U., "Echolocation Signals of the Greater Horseshoe Bat (*Rhinolophusferrumequinum*) in Transfer Flight and During Landing," *Journal of Acoustical Society of America*, Vol. 101, No. 4, April 1997, pp. 2347–2364.

[15] Hiryu, S., Katsura, K., Lin, L., Riquimaroux, H., and Watanabe, Y., "Doppler-Shift Compensation in the Taiwanese Leaf-Nosed Bat (*Hipposideros Terasensis*) Recorded with a Telemetry Microphone System During Flight," *Journal of Acoustical Society of America*, Vol. 118, No. 6, Dec. 2005, pp. 3927–3933.

[16] Oh, S.-R., Pathak, K., Agrawal, S., Pota, H., and Garrett, M., "Autonomous Helicopter Landing on a Moving Platform Using a Tether," *IEEE International Conference on Robotics and Automation*, IEEE, Piscataway, NJ, April 2005, pp. 3960–3965.

[17] Valenti, M., Bethke, B., Fiore, G., How, J., and Feron, E., "Indoor Multi-Vehicle Flight Testbed for Fault Isolation, Detection and Recovery," AIAA Paper 2006-6200, Aug. 2006, pp. 98–108.

[18] Gavrilets, V., Mettler, B., Frazzoli, E., Piedmonte, M., and Feron, E., "Aggressive Maneuvering of Small Autonomous Helicopters: A Human-Centered Approach," *International Journal of Robotics Research*, Vol. 20, No. 10, Oct. 2001, pp. 795–807. doi:10.1177/02783640122068100

[19] Gavrilets, V., Mettler, B., and Feron, E., "Human-Inspired Control Logic for Automated Maneuvering of a Miniature Helicopter," *Journal of Guidance, Control, and Dynamics*, Vol. 27, No. 5, 2004, pp. 752–759. doi:10.2514/1.8980

[20] Abbeel, P., Coates, A., Quigley, M., and Ng, A., "An Application of Reinforcement Learning to Aerobatic Helicopter Flight," *Proceedings of the Neural Information Processing Systems Conference*, MIT Press, Cambridge, MA, 2007, pp. 1–8.

[21] Ng, A., Coates, A., Diel, M., Ganapathi, V., Schulte, J., Tse, B., Berger, E., and Liang, E., "Inverted Autonomous Helicopter Flight via Reinforcement Learning," *Proceedings of the International Symposium*

on Experimental Robotics, Springer Tracts in Advanced Robotics, Springer, Berlin/Heidelberg, 2006, pp. 363–372.
[22] Gavrilets, V., Mettler, B., and Feron, E., "Control Logic for Automated Aerobatic Flight of a Miniature Helicopter," AIAA Paper 2002-4834, Aug. 2002.
[23] Von Mises, R., *Theory of Flight*, Dover Publications, New York, 1959, p. 100.
[24] Hoerner, S., *Fluid Dynamic Drag*, *Hoerner Fluid Dynamics*, Bakersfield, CA, 1965, Chap. VI.
[25] Padfield, G., *Helicopter Flight Dynamics*, AIAA Education Series, AIAA, Washington, D.C., 1995.
[26] Khalil, H., *Nonlinear Systems*, 3rd ed., Prentice–Hall, Upper Saddle River, NJ, 2002.
[27] Nelson, R., *Flight Stability and Automatic Control*, McGraw–Hill, New York, 1998, p. 103.
[28] Murray, R., Li, Z., and Sastry, S., *A Mathematical Introduction to Robotic Manipulation*, CRC Press, Boca Raton, FL, 1993, p. 413.
[29] Frazzoli, E., Dahleh, M., and Feron, E., "Trajectory Tracking Control Design for Autonomous Helicopters Using a Backstepping Algorithm," *Proceedings of the American Control Conference*, IEEE, Piscataway, NJ, June 2000, pp. 4102–4107.